Chemistry Faculty Research & Creative Works

Chemistry

01 Jan 2011

Enhanced Photorefractivity in a Polymeric Composite Photosensitized with Carbon Nanotubes Grafted to a Photoconductive Polymer

Naveen Kumar Lingam

Sonali Kalghatgi

Jeffrey G. Winiarz
Missouri University of Science and Technology, winiarzj@mst.edu

Follow this and additional works at: https://scholarsmine.mst.edu/chem_facwork

Part of the Chemistry Commons

Recommended Citation

Enhanced photorefractivity in a polymeric composite photosensitized with carbon nanotubes grafted to a photoconductive polymer

Naveen K. Lingam, Sonali Kalghatgi, and Jeffrey G. Winiarz[a]
Department of Chemistry, Missouri University of Science and Technology, Rolla, Missouri 65409, USA

We report on the photosensitization of photorefractive (PR) polymeric composites through the inclusion of multiwalled and singlewalled carbon nanotubes (CNTs), respectively, having poly(*N*-vinyl carbazole) (PVK) grafted to their surfaces. The PR nature of the holographic gratings was confirmed via the asymmetric exchange of energy in a two-beam-coupling (TBC) geometry, yielding TBC gain coefficients approaching 80 cm^{-1}. In addition, in degenerate-four-wave-mixing experiments the prepared composites exhibited diffraction efficiencies as high as 60% and overmodulation voltages as low as $\sim$40 V/μm. These notable figures of merit indicate that the grafting of the PVK polymer to the various CNTs results in enhanced PR performance. The mechanism responsible for this enhancement in PR performance is investigated using a variety of experimental techniques. © *2011 American Institute of Physics*. [doi:10.1063/1.3530583]

I. INTRODUCTION

Due to their unique optical and electronic properties, carbon nanotubes (CNTs) have recently been the subject of many studies involving a variety of applications, especially those concerning photoluminescence, electroluminescence, optical power limiting, Raman scattering, and photoconductivity (PC).[1–13] Since PC, along with electro-optic activity, is a necessary component of the photorefractive (PR) effect, it follows that CNTs may function as the photosensitizer in PR polymeric composites. Polymeric PR composites are known for their large optical nonlinearities, low permittivity, and low cost, and are potentially useful in a variety of real-time optical information processing functions including beam clean-up and amplification, dynamic interferometry, phase conjugation, and pattern recognition.[14–18] Consequently, much research has been directed toward the advancement of this class of materials, resulting in significant progress including millisecond response times and nearly 100% diffraction efficiencies.[16,17] Despite this success, all-organic PR composites suffer from limited spectral sensitivity. While several dopants have been identified which effectively photosensitize organic PR composites with respect to visible wavelengths, most notably C$_{60}$, none have been discovered which operate efficiently in the technologically important IR wavelengths. With regard to CNTs, their associated broadband absorption is especially appealing as it allows for the possible photosensitization of PR composites across the visible spectrum as well as at the technologically important NIR wavelengths. This has motivated several studies in which CNTs have been doped into PR polymer composites to act as the photosensitizer.[19–25] In perhaps the most notable of these studies (λ=1064 nm), maximum degenerate-four-wave-mixing (DFWM) efficiencies of approaching 1.5% and two-beam-coupling (TBC) gain coefficients of 84 cm^{-1} were reported.[24] Although significant, these figures of merit leave much room for improvement.

Recent research has demonstrated the ability to covalently bond the poly(*N*-vinyl carbazole (PVK) polymer to the surface of CNTs.[2,6,26–30] It is anticipated that by covalently bonding the charge-generating CNTs and the charge-transporting PVK polymer, the solubility of the CNTs within the polymeric matrix may be improved, resulting in enhanced PR performance. It is well known that CNTs are extremely insoluble in virtually all traditional organic solvents. This relative insolubility has been shown to also apply to solid polymeric systems, in which phase separation is observed as the nanotubes segregate into black crystalline formations.[25] Phase separation detrimentally affects the optical quality of the PR composite, and since the PR effect is activated through the interference of two intersecting coherent laser beams, the importance of the sample's optical quality cannot be over emphasized. A second advantage gained from the covalent bonding of the PVK polymer to the CNTs is the ensuing intimate contact between the CNT and the PVK molecule, resulting directly from the formation of the covalent bond. It is well-known that such chemical bonding between species greatly promotes the charge-transfer process, a process which in this case is required to initiate the PR mechanism. Therefore, the enhanced efficiency associated with the transfer of free charge-carriers from the photosensitizing CNT to the charge-transporting PVK matrix should result in enhanced PR performance.

II. EXPERIMENTAL DETAILS

Dichlorobenzene (DCB), 70% HNO$_3$ aqueous solution, tetrahdrofuran (THF), ethanol (EtOH), methanol (MeOH), azo-bis-isobutyronitrile (AIBN), and tritolylphosphate (TCP), were purchased from Aldrich as used as received. PVK ($\bar{M}_n$=4.2×10^4; $\bar{M}_w$/$\bar{M}_n$$\sim$2) was purchased from Aldrich and purified by dissolving in THF and subsequently dripping the solution into EtOH thus precipitating the PVK which was then collected by filtration and washed with excess EtOH. The nonlinear optical dye, 2-(4-azepan-1-yl-

a)Electronic mail: winiarzj@mst.edu.

TABLE I. Compositions of the various PR devices used in this study.

Device	PVK (wt %)	TCP (wt %)	7-DCST (wt %)	CNT (wt %)	Grafted PVK (wt %)
M1	49.9	15.0	34.9	6.65×10^{-3}	0.242
M3	49.6	14.9	34.7	2.20×10^{-2}	0.801
M10	48.8	14.6	34.1	6.51×10^{-2}	2.37
UM3	50.0	15.0	35.0	2.22×10^{-2}	N/A
S1	50.0	15.0	35.0	1.27×10^{-2}	2.16×10^{-2}
S3	49.9	15.0	35.0	4.22×10^{-2}	7.19×10^{-2}
S10	49.8	14.9	34.9	0.126	0.215
U.S.3	50.0	15.0	35.0	4.23×10^{-2}	N/A
C0	50.0	15.0	35.0	N/A	N/A

benzylidene)-malononitrile (7-DCST) was synthesized in our laboratory based on procedures described in the literature.[31,32] Multiwalled CNTs (MWCNTs) (length $=5-20$ μm, OD$=15 \pm 5$ nm, purity$>95\%$) and single-walled CNTs (SWCNTs) (length$=>10$ μm, OD $=1-1.5$ nm, purity$>40\%$) were purchased from NANOLAB and purified prior to use as described in the literature.[2] The company which supplied the CNTs reports that the as-purchased SWCNTs and MWCNTs are $\sim60\%$ semiconducting with the remainder being metallic in nature. No effort was made to modify this ratio. To clean the CNTs, 100 mg of either MWCNTs or SWCNTs were introduced into a three-neck round bottom flask. Subsequently, 28.5 ml of 70% HNO$_3$ aqueous solution and 71.5 ml of distilled water were added and the solution was refluxed for 18 h with magnetic stirring. Upon cooling to room temperature, the solution was diluted with 200 ml of distilled water and the solid precipitate was collected by vacuum filtration and washed with distilled water until a neutral pH was observed. The product was then dried at room temperature under vacuum for several days until a free-flowing black powder was obtained.

Grafting of the PVK onto the SWCNTs and MWCNTs was conducted using a procedure described in the literature for grafting of PVK to MWCNTs and was appropriately tailored for the grafting of the PVK to SWCNTs.[2] All manipulations were conducted under nitrogen employing standard Schlenk techniques. Initially, 100 mg of acid-purified CNTs and 10 ml of DCB were charged in a round bottom flask and sonicated for ~30 min. In a separate container, 200 mg of PVK and 22 mg of AIBN were dissolved in 10 ml of DCB and this solution was added to the CNT solution. The mixture was stirred at room temperature for several hours until a homogenous black suspension was observed. At this time, the solution was refluxed at 70 °C for ~48 h. The mixture was then cooled to room temperature and an additional 100 ml of DCB was added, and the diluted mixture was sonicated for 1 h. The product was precipitated through the addition of a minimum amount of MeOH, collected via centrifugation, and redispersed in toluene. This process was repeated several times in order to remove any unreacted PVK or AIBN. The obtained product was then again washed with EtOH, collected, and dispersed in toluene. Any solid which would not dissolve in the toluene was collected by centrifugation and discarded. The PVK grafted CNTs (PVK-CNT) dispersed in toluene were characterized and used in the fabrication of PR

devices. The PVK:CNT mass ratio associated with the final product could be determined spectroscopically. Here, we first constructed a calibration curve, devised by measuring the absorption of several solutions of known concentration of acid-purified CNTs in toluene. Then a known mass of PVK-CNT was dissolved in toluene and the mass of the CNTs contained within the solution could be determined based on the optical absorption of the solution in conjunction with the described calibration curve. It was then assumed that the difference between the masses represented the mass of the grafted PVK.

The various PR devices were prepared by first dissolving known masses of PVK, TCP, and 7-DCST in toluene. To this mixture, a known concentration and volume of PVK-CNT dissolved in toluene was added and the mixture was filtered to eliminate any undissolved solids. The solution was then stored in a vacuum oven at 50 °C for 24 h to remove the solvent. The solid residue was subsequently recovered, placed between two pieces of glass coated with indium tin oxide and heated above its melting temperature on a hotplate. The PR device was then mechanically pressed forming the typical "sandwich" geometry using glass spacers to control the thickness of the device, d, at 100 μm. In an effort to optimize the PR performance, a large matrix of device compositions were sampled, however, here we will present the results only for those device compositions at or near the optimized concentration of PVK-CNT. As such, the findings for three compositions photosensitized with MWCNTs and three compositions photosensitized with SWCNTs will be presented. In addition to the six devices photosensitized with PVK-CNT, a series of control devices were also fabricated. The compositions of all devices are presented in Table I and the experimentally measured absorption coefficients at λ $=633$ nm, α_{633}, are given in Table II. For all PR devices, the PVK:7-DCST:TCP ratio was held constant, with the exception of the relatively insignificant amount of additional PVK grafted to the surface of the CNTs. The PR devices have not shown any change in their optical properties or degradation in PR performance over the course of 6 months.

All optical characterizations were conducted with λ $=633$ nm unless otherwise noted. The PR properties of the composite devices were studied via TBC and DFWM techniques using a standard tilted geometry. Holographic gratings were written through the intersection of two coherent beams generated by a helium-neon laser operating with incident

TABLE II. Optical quality, α_{633}, Γ_{max}(cm^{-1}), $\eta_{int,max}$, $\eta_{ext,max}$ of the various PR devices used in this study.

Device	Optical quality	α_{633} (cm^{-1})	Γ_{max} (cm^{-1})	$\eta_{int,max}$	$\eta_{ext,max}$
M1	Excellent	6.71	31.7	0.509	0.422
M3	Excellent	11.1	78.1	0.599	0.438
M10	Slightly hazy	29.7	2.16	0.480	0.208
UM3	Opaque	N/A	N/A	N/A	N/A
S1	Excellent	6.50	14.7	0.301	0.251
S3	Slightly hazy	17.4	3.60	0.421	0.258
S10	Very hazy	37.9	N/A	N/A	N/A
U.S.3	Opaque	N/A	N/A	N/A	N/A
C0	Excellent	4.30	0.00	0.00	0.00

angles of $\theta_1=45°$ and $\theta_2=75°$ (in air) relative to the sample normal. In the TBC experiments, both writing beams were p-polarized with intensities of $I_1 \sim 0.04$ mW and $I_2 \sim 6$ mW. The external bias was applied such that I_1 would experience gain at the expense of I_2. Asymmetric energy transfer was observed by monitoring the intensities of the writing beams after the PR device with a photodiode. In the DFWM experiment the writing beams were s-polarized with intensities of $I_1 \sim 3$ mW and $I_2 \sim 7$ mW. In addition, a p-polarized probe beam propagated in a direction opposite to I_1 with an intensity of $I_p \sim 3$ μW. Through the use of a polarizing beam splitter placed in the path of I_2 in conjunction with a photodiode, the diffracted portion of I_p, also referred to as the signal beam, I_s, could be quantified. In all PR experiments, I_1 and I_2 had beam diameters of ~ 280 μm while I_p possessed a beam diameter of ~ 120 μm. Beam diameters were measured by using a fractional irradiance of $1/e^2$.

PC, σ_p, characterizations were made with a dc-photocurrent technique using a Keithley electrometer to measure the current passing through the PR device as a function of applied bias. The beam intensities for all σ_p characterizations were ~ 11 mW with a beam diameter of 0.98 mm. This technique also permits the measurement of the dark conductivities, σ_d, associated with the PR devices.

Visible absorption spectra were recorded on a Beckman DU 640B spectrophotometer. The absorption spectra of the PVK-CNT suspensions were obtained using a 1 cm quartz cell at concentrations of ~ 0.01 mg/ml of CNTs in toluene.

III. RESULTS AND DISCUSSION

The PVK-CNTs utilized in this study were synthesized based on a procedure found in the literature.[2] The initial step concerned the purification of the SWCNTs and the MWCNTs using an HNO$_3$ bath, in each case producing a free-flowing powder which was deep black in color. In order to quantify the CNT concentration of solutions used in preparation of the PR devices, calibration curves were constructed by dissolving known masses of acid-washed CNTs in toluene and measuring the optical absorption of the various concentrations. It was determined from the slope, m, of a linear least-squares fit to the data that the acid-purified MWCNTs had an absorption of 46 ± 1.3 lg^{-1} cm^{-1} whereas the acid-purified SWCNTs had an absorption of 24 ± 0.010 lg^{-1} cm^{-1} (see Ref. 43) for a graphical representation of the least-squares fit). The acid-washed CNTs exhibited relatively poor solubility in most common organic solvents, and concentrations exceeding ~ 0.02 mg/ml in toluene resulted in rapid aggregation of the CNTs. This was especially true for the acid washed SWCNTs.

The next step in our procedure involved the grafting of the PVK to the CNTs. As described in the experimental section, extreme care was taken in ensuring complete removal of unreacted PVK, CNT and AIBN upon the conclusion of this procedure. After synthesis of respective PVK-CNTs, the solvent was removed under vacuum and, in the case of the PVK-MWCNT, a light gray powder was recovered. In contrast, removal of the solvent from the PVK-SWCNT yielded a dark black powder. This difference in color indicates that significantly more PVK was successfully grafted to the surface of the MWCNTs as compared to the surface of the SWCNTs. It is speculated that this is the reason why the literature source for this synthesis involves MWCNTs but not SWCNTs.[2] Why PVK is more effectively grafted to MWCNTs than it is to SWCNTs is the subject of future studies. Visible absorption spectra were obtained for the PVK-SWCNT and PVK-MWCNT solvated in toluene in a 1 cm cell and are presented in Fig. 1. Both spectra are normalized to 1 mg of CNT per milliliter of solution. The absorption spectra obtained for PVK-CNT were qualitatively identical to those obtained for the unadorned acid-washed CNTs at similar concentrations (not shown). In order to quantitatively determine the PVK/CNT mass ratio of the dried PVK-CNT powders, a known mass of PVK-CNT powder was dissolved in a known volume of toluene. By obtaining an absorption spectrum of the solvated PVK-CNT, it was possible to determine the concentration, and hence the mass, of CNTs in the solution. The difference between the spectroscopically determined mass of the CNT and the known mass of the dissolved PVK-CNT was attributed to the mass of the grafted PVK. For the grafted samples, the PVK/MWCNT mass ratio was determined to be 36.4 whereas the PVK/SWCNT mass ratio was established as 1.70. This result supports the conclusion that the difference in color between the gray PVK-MWCNT powder and the dark black PVK-SWCNT powder is due to the difference in the amount of PVK which was successfully grafted to the respective CNT
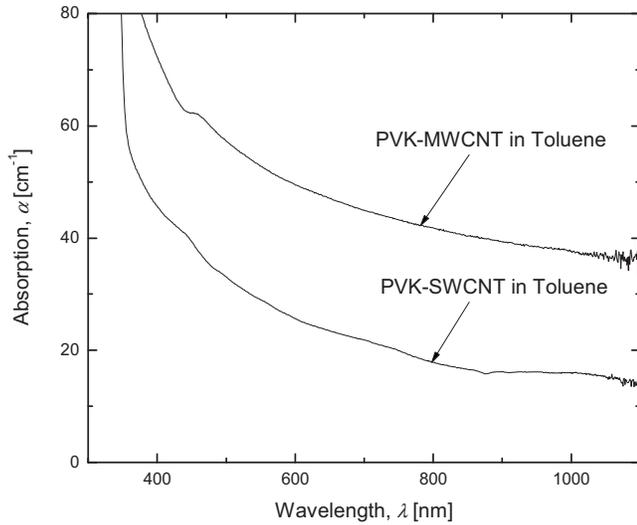
FIG. 1. Absorption spectra of the grafted PVK-MWCNT and PVK-SWCNT in toluene. The spectra are normalized to represent a concentration of 1 mg/ml of the CNT and not the additional mass associated with the grafted PVK.
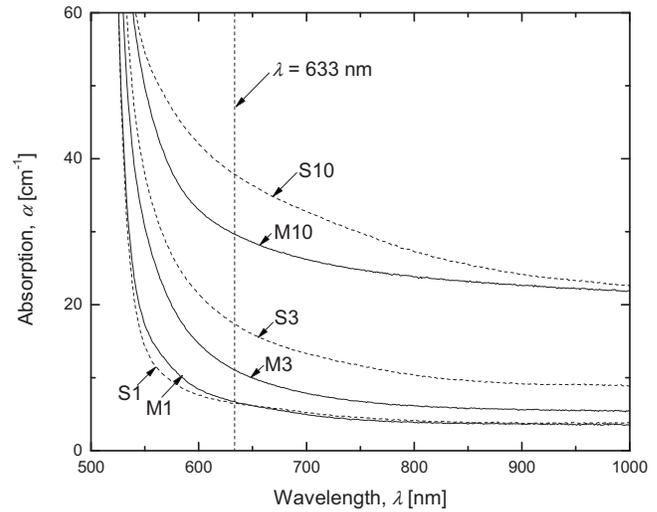

FIG. 2. Absorption spectra of the PVK-MWCNT photosensitized PR devices (solid lines) and the PVK-SWCNT photosensitized PR devices (dashed lines) used in this study.

surfaces. The spectroscopic data does not indicate the formation of a charge-transfer complex between the CNTs and the PVK.

PR devices were fabricated using PVK-MWCNT and PVK-SWCNT as the photosensitizer. The composites used in this study consisted of the same constituents in approximately the same concentrations, with the exception of the PVK-CNT photosensitizer. The basic components used in each composite were PVK:7-DCST:TCP, blended with a standard mass ratio of 50:35:15. Here, PVK is a hole-transporting photoconductive polymer and is commonly used for this purpose in PR composites.[16,17] Modulation of the refractive index is accomplished through the inclusion of the nonlinear optical (NLO) dye, 7-DCST. Finally TCP functions as an inert plasticizer, permitting room-temperature poling of the NLO dye. For this study we intended to fabricate two series of PR devices; the first consisting of three PR devices photosensitized through the inclusion of PVK-MWCNT and the second set of three PR devices photosensitized through the inclusion of PVK-SWCNT, varying the concentration of the PVK-CNT used in each series so as to optimize the PR performance within each series. Therefore, the first composite, labeled as M1, was fabricated by adding 0.0133 mg of MWCNT associated with 0.485 mg of grafted PVK to 200 mg of PVK:7-DCST:TCP in the standard mass ratio, yielding a composition detailed in Table I. The next composite was similar in composition to that of M1, with the exception that the amount of PVK-MWCNT added to the standard components was three times that added to the M1 composite, as such, devices fabricated from this composite were labeled as M3. The final composite photosensitized with PVK-MWCNT was again similar in composition to that of M1, with the exception that the amount of PVK-MWCNT was increased by a factor of 10, and devices fabricated from this composite are labeled as M10. The compositions of the M3 and M10 PR devices are detailed in Table I and the α_{633} for all PR devices are specified in Table II. In a similar fashion,

a series of PR devices labeled as S1, S3, and S10 were fabricated using PVK-SWCNT as the photosensitizer. The precise compositions of the PVK-SWCNT photosensitized PR devices are given in Table I and their respective α_{633} are reported in Table II. The visible absorption spectra of the aforementioned PR devices ($d = 100$ μm) are presented in Fig. 2. Evident in the figure is that as the concentration of the PVK-SWCNT is increased, the α_{633} becomes increasingly larger than would be anticipated based solely on absorption considerations. It has been confirmed through inspection with a conventional optical microscope as well as light-scattering experiments that this is due to aggregation of the PVK-SWCNT within the solid composite. This increased propensity for aggregation, relative to PVK-MWCNT photosensitized devices, is due to the decreased amount of PVK which was successfully grafted to the SWCNTs as compared to that of the MWCNTs. A qualitative description of the optical quality associated with each PR device is provided in Table II.

In addition to the PVK-CNT photosensitized PR devices, several control devices were fabricated. First, we fabricated a PR device void of any photosensitizing species and consisting only of PVK:7-DCST:TCP in the standard mass ratio, as illustrated in Table I and referred to herein as the C0 PR device. As revealed in Table II, the C0 PR device exhibited $\alpha_{633} \approx 4.3$ cm^{-1}. A plot of α_{633} versus CNT concentration for the M1, M3, and M10 series of PR devices yielded a straight line with a y-intercept/cm^{-1} of 4.05 ± 0.92, corresponding to 0 wt % of MWCNT, in good agreement with to the 4.3 cm^{-1} value measured for the unsensitized C0 device. A similar plot was constructed for the PVK-SWCNT photosensitized devices and despite the optical scattering associated with the S3 device, and especially the S10 device (as evidenced in Fig. 2), a plot of the α_{633} versus PVK-SWCNT concentration for the three devices nevertheless resulted in a y-intercept/cm^{-1} of 4.32 ± 2.0, again corresponding well to the anticipated value of 4.3 cm^{-1}. See Ref. 43 for the plots of the α_{633} as a function of CNT concentration for each se-

ries of CNT photosensized devices. It is also noted that despite the relatively successful grafting of the PVK to the MWCNT, some aggregation was present in M10 in the form of a slight haziness observed for the device film.

In addition to the unsensitized control device, two more control devices were fabricated. Here we photosensitized the PVK:7-DCST:TCP with acid-washed MWCNTs and SWCNTs which did not have PVK grafted to their surface, and refer to these PR devices as CM3 and CS3, respectively. As will be seen, for PVK-MWCNT photosensitized devices, it was M3 which demonstrated the best PR performance. For this reason, CM3 was fabricated such it had the same concentration of MWCNTs as the M3 device, however lacking the grafted PVK. For similar reasoning, CS3 contains the same SWCNT concentration as that of S3, but again, lacking any grafted PVK. As described in Table II, CM3 and CS3 exhibited such severe phase separation that they were completely opaque under practical experimental conditions.

It is interesting to note that preliminary studies related to this work involved the screening of other charge-transporting species in addition to PVK. Most notably we attempted to utilize N,N′-diphenyl-N,N′-bis(3-methylphenyl)-[1,1′-biphenyl]-4,4′-diamine (TPD), derivatives which have shown to exhibit a performance superior to that of PVK in some circumstances.[33–40] In this case however, PR devices using TPD as the charge-transporting species showed markedly diminished performance when compared to analogous devices employing PVK. To account for this, it is supposed that although charge-generation occurs within the CNT, in due course the hole becomes associated with a grafted PVK molecule. From here it may recombine with the electron or may dissociate from the grafted PVK molecule, and associate with a PVK molecule which is part of the larger charge-transport matrix, at which time it may further go on to contribute to the PR space-charge field. The enhanced charge-transfer associated with the PVK matrix is likely attributable to an enhanced intermingling between the CNT-grafted-PVK and the PVK composing the charge-transport matrix.

The PR nature of the gratings created within the composites used in this study could be confirmed using conventional TBC experiments. A unique feature of the PR effect is that the refractive index grating created in the medium is spatially shifted with respect to the light intensity pattern of the interfering writing beams, resulting in an asymmetric exchange of energy between the beams interfering in the PR medium.[16,41] The TBC gain coefficient, Γ, is given in terms of the experimentally measured quantities γ_0 and β, as

$$\Gamma = \frac{1}{L}[\ln(\gamma_0\beta) - \ln(\beta + 1 - \gamma_0)], \tag{1}$$

where L is the path length of the beam experiencing gain inside the PR device, β is the ratio of the writing beam intensities before the PR device, and γ_0 is the ratio of the intensity of the beam experiencing gain with and without the pump beam. For the composites investigated here, the TBC gain coefficients at $\lambda = 633$ nm, Γ_{633}, as a function of the externally applied electric field, E, are presented in Fig. 3. Immediately apparent in the figure is the absence of data for S10. Despite several attempts to fabricate devices of S10
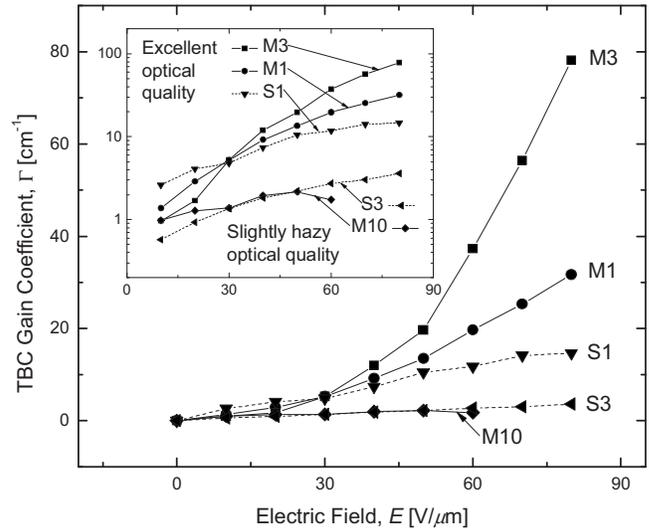

FIG. 3. Two beam coupling gain coefficient, Γ_{633}, as a function of the externally applied electric field, E. The inset depicts the same data on a log plot. The lines are guides for the eye.

composition, all S10 devices experienced dielectric breakdown below 30 V/μm and more typically <20 V/μm. Consequently, further data was not obtained for this composition. As acknowledged in Table II, aggregation of the PVK-SWCNT was visibly evident in the S10 devices resulting in a very hazy optical quality. Clearly, severe aggregation of the PVK-CNT also strictly limits the magnitude of E which the device can withstand prior to breakdown. Similar behavior was observed for the slightly hazy M10, however, to a significantly lesser degree, which could typically withstand E =60 V/μm prior to dielectric breakdown. While PR devices fabricated from the S3 composite exhibited a slightly hazy optical quality, comparable to that observed for M10, S3 regularly withstood E=80 V/μm, which was the maximum E used in this study. The control devices CM3 and CS3 were sufficiently conductive that a measurable E could not be established and therefore data could not be obtained for these devices. The high conductivity associated with these composites is attributed to the extremely large aggregates of unadorned CNTs present in the films. The control device C0 did not exhibit a measurable TBC signal. Given that the CNTs used in this study are relatively long ($\sim$20 μm) in comparison to device thickness (d=100 μm), there was initial speculation that this dimensional similarity may result in charge-transport through the CNTs, and subsequent electrical shortage of the PR device. However, provided the concentration of the CNTs was maintained below that which gave way to visible aggregation, this adverse behavior was not observed and PR devices exhibiting high optical quality were also extremely robust with regard to withstanding the higher E.

Evident from Fig. 3, and specified in Table II, M3 demonstrated the best TBC performance with Γ_{633}=78.1 cm^{-1} at E=80 V/μm. Succeeding M3 in TBC performance was M1, with Γ_{633}=31.7 cm^{-1}. Compared to M1, M3 had $\sim$3$\times$ the concentration of the photosensitizing PVK-MWCNT species, and so the relative improvement in TBC performance was not unexpected. This trend does not continue beyond the

concentration associated with M3 however, with M10 exhibiting a maximum $\Gamma_{633}=2.16$ cm^{-1}. This dramatic decrease in TBC performance is attributed to the decrease in the optical quality of the PR device, resulting from the relatively high concentration of PVK-MWCNT. With respect to the PR devices photosensitized via the inclusion of PVK-SWCNT, S1 exhibited the superior performance with a maximum $\Gamma_{633}=14.7$ cm^{-1}. Although S3 contained a higher concentration of PVK-SWCNT, the low degree of PVK grafted to the SWCNT surface resulted in aggregation, and subsequently a visible degradation in the optical quality. Accordingly, a relative decrease in TBC performance was observed with a maximum $\Gamma_{633}=3.60$ cm^{-1}. The consequence of the deterioration in optical quality is more apparent in the inset of Fig. 3, where the identical data are presented on a log plot. Here, two distinct groupings of data are apparent, with each grouping characterized by its optical quality. Summarizing the TBC data, it is apparent that the Γ_{633} for CNT photosensitized PR devices shows continual improvement until such time that aggregation of the PVK-CNT starts to adversely affect the optical quality of the PR device, where the Γ_{633} exhibits a dramatic decrease. Moreover, PR devices photosensitized with PVK-MWCNTs show superior performance when compared to those PR devices photosensitized through the inclusion of PVK-SWCNTs.

For practical applications, the optical amplification, Γ_{633}, should exceed the absorption, α_{633}, for a given device. As evident from Table II, this is the case for all tested devices with the exception of M10 and S3. The best performance in this regard was again observed for M3 with $\Gamma_{633}-\alpha_{633}=67.0$ cm^{-1}. Furthermore, for this composite $\Gamma_{633}>\alpha_{633}$ when $E>\sim40$ V μm. The observation of optical amplification at such a low E indicates the potential for using PVK-CNT photosensitized composites for various practical applications.

Having confirmed the PR nature of the diffraction gratings, the internal diffraction efficiencies, η_{int}, were measured in a DFWM experiment and quantified according to the equation

$$\eta_{int}=\frac{I_s}{I_p'}, \tag{2}$$

where I_p' is the intensity of the probe beam after the device with $E=0$ V and I_s is the intensity of the diffracted portion of I_p with $E\neq0$ V. The measured η_{int} as a function of E are depicted in Fig. 4 for the relevant compositions. The solid lines in the figure represent the best fit of the data to the function

$$\eta=\sin^2(C\Delta n), \tag{3}$$

where Δn is the modulation in refractive index and C is a geometric constant.[16,41] Illustrated in the figure and quantified in Table II, the greatest internal DFWM efficiency was exhibited by M3 with $\eta_{int,max}=59.9\%$ at the overmodulation voltage of ~50 V/μm. It is noted that this diffraction efficiency is considerably larger than any other reported for a PR device photosensitized through the inclusion of CNTs, and attributable to the grafting of the PVK to the CNTs. Unlike the TBC, the DFWM efficiency is evidently not as sensitive
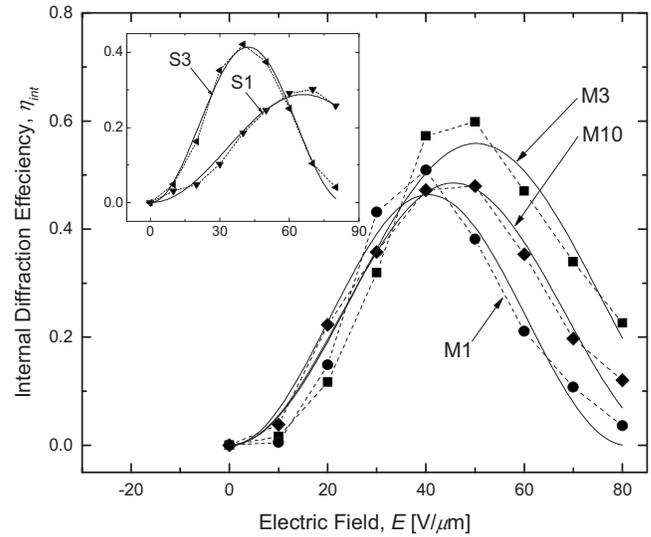

FIG. 4. Internal diffraction efficiencies, η_{int}, as a function of the externally applied electric field, E. The dashed lines are guides for the eye and the solid lines represent functional fits to the data.

to the optical quality of the device, with M1 and M10 showing very similar efficiencies of $\eta_{int}\approx50\%$. Although diminished relative to M3, these η_{int} are nevertheless greatly improved relative to previous reports pertaining to ungrafted CNTs. In looking at the DFWM performance of the PVK-SWCNT photosensitized PR devices, depicted in the inset of Fig. 4, we again witness the apparent insensitivity to the diminished optical quality as S3, with its higher PVK-SWCNT content, exhibits a slightly better performance than that associated with S1. In addition to the observed improvement with regard to efficiency, a reduction in the overmodulation voltage is also realized, decreasing from ~70 to ~40 V/μm. The performance associated the PVK-SWCNT photosensitized PR composites are notably inferior relative to those containing PVK-MWCNT. We initially attributed this disparity to the difference between the charge generation quantum-efficiencies associated with the well-grafted PVK-MWCNTs compared to the relatively unadorned PVK-SWCNTs. PC characterizations, which are subsequently detailed, indicate a more multifaceted rationalization.

While the internal diffraction efficiencies are of fundamental importance, it is the external diffraction efficiencies, η_{ext}, which convey practical merit. Here η_{ext}, accounting for reflections, was determined according to the equation

$$\eta_{ext}=\frac{I_s}{I_p}, \tag{4}$$

where I_p is the intensity of the probe beam before the device. The calculated $\eta_{ext,max}$ are presented in Table II where it is evident that M3 retains its dominance with regard to performance despite its higher α_{633} relative to M1. The high α_{633} associated with M10 causes its $\eta_{ext,max}$ to be significantly diminished relative to those of M1 and M3. With regard to the PVK-SWCNT photosensitized devices, we see that the lower absorption coefficient associated with S1 has resulted in a $\eta_{ext,max}$ which approaches that of the S3 device. See Ref. 43 for the η_{ext} as a function of E.
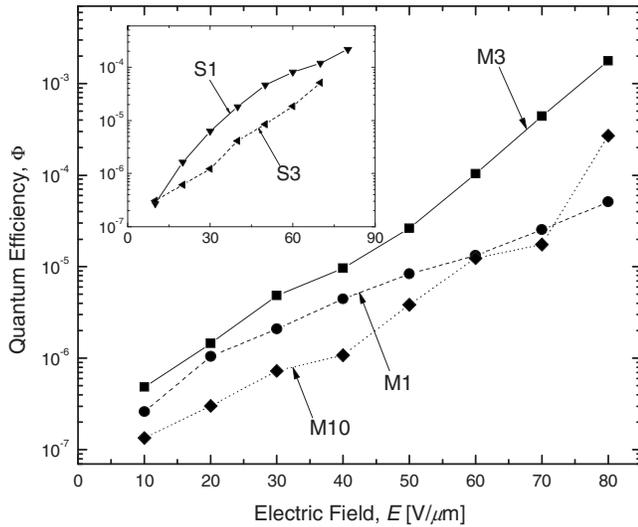
FIG. 5. Quantum efficiency, Φ, as a function of the externally applied electric field, E. The lines are guides for the eye.

FIG. 6. Ratio of the photoconductivities to the dark-conductivity, σ_p/σ_d, as a function of the externally applied electric field, E. The lines are guides for the eye.

As described, the superior PR performance associated with the PVK-MWCNT photosensitized devices over their PVK-SWCNT photosensitized counterparts was anticipated. This speculation was based on the larger extent to which PVK which could be successfully grafted to the surfaces of the different CNTs. As a result of the MWCNTs being more heavily adorned with PVK molecules, it was anticipated that this would result in a greater solubility of the CNT and a greater intermingling between the hole-intermediating grafted PVK and the PVK composing the charge-transporting matrix. In order to assess this argument, conductivity experiments were conducted using a dc-photocurrent experiment in which the current passing through the device could be monitored with or without illumination (λ =633 nm). Using this technique it is possible to evaluate the composites in terms of their charge-generation quantum efficiencies, Φ, using the equation

$$\Phi = \frac{N_{cc}}{N_{ph}} = \frac{J_p hc}{I\lambda e \alpha_\lambda d}, \tag{5}$$

where N_{cc} is the number of charge-carriers generated per unit volume, N_{ph} is the number of photons absorbed per unit volume, h is Plank's constant, c is the speed of light, e is the fundamental unit charge, and J_p is the current density in the device under illumination of intensity, I. The Φ measured for the devices used in this study are depicted as a function of E in Fig. 5. As seen in the figure, the difference in Φ among the various composites is small, however, some trends are evident. It is observed that an increase the PVK-MWCNT concentration of in going from M1 to M3 results in an improved Φ. The exact reason for this observation is not immediately clear but reveals that the charge-generation process in these composites is not as straightforward as initially assumed. Specifically, this observation indicates that the probability of an absorbed photon converting into a free charge-carrier is dependent upon the environment of the PVK-CNT, and apparently the proximity of another PVK-CNT. In contradiction to this trend, it is observed that the further increase in PVK-MWCNT concentration in going from M3 to M10 re-
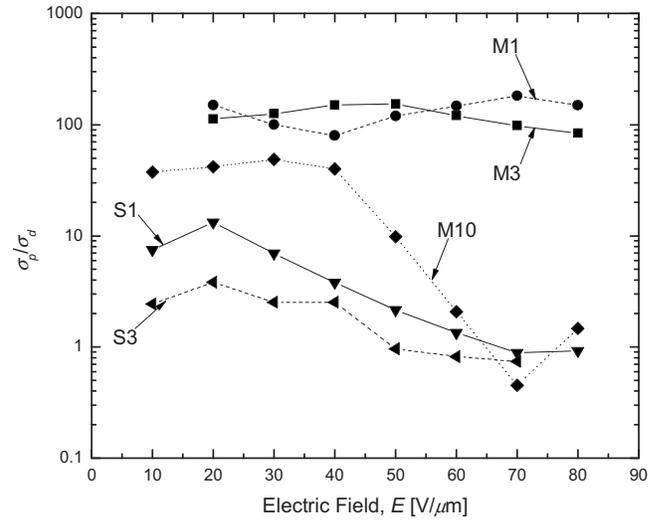
sults in a decreased Φ. This indicates that the slight amount of aggregation observed in M10 can significantly affect the ability of the PVK-MWCNT to inject charge-carriers into the charge-transporting matrix. It is also interesting to note that the Φ measured for the M1 and S1 composites were nearly the same. In contrast to initial speculation, this observation indicates that the intermingling between the grafted PVK and the PVK matrix may not be as significant with regard to charge separation as initially supposed. The increase in the PVK-SWCNT concentration in going from the S1 device to the S3 device, a decrease in Φ is observed. Due to the slight degree of aggregation observed in the S3 device, and based on the trends seen in the PVK-MWCNT photosensitized series of devices, this outcome was predicted. While some of the trends observed in Φ could be correlated with the differences in the PR performance, it is still not immediately clear why the PR performance of the PVK-MWCNT photosensitized composites were significantly better than those photosensitized through the inclusion of PVK-SWCNT. As such, further analysis was conducted. See Ref. 43 for the photosensitivity as a function of E.

Relevant to the PR performance of a polymeric device is the ratio of the PC, σ_p, to the dark-conductivity, σ_d, σ_p/σ_d, as revealed from the equation

$$E_{sc} = G(E)\left[1 + \left(\frac{\sigma_d}{\sigma_p}\right)\right]^{-1}, \tag{6}$$

where E_{sc} is magnitude on the internal PR space-charge field and $G(E)$ depends on the external E as well as experimental parameters.[16,41] Here, the conductivities, σ, were calculated according to the equation

$$\sigma = \frac{J}{E}, \tag{7}$$

where J is the current density with or without illumination. The σ_p/σ_d data are plotted as a function of E for the various composites in Fig. 6 and are useful in discerning the differences in PR performance between the PVK-MWCNT photo-
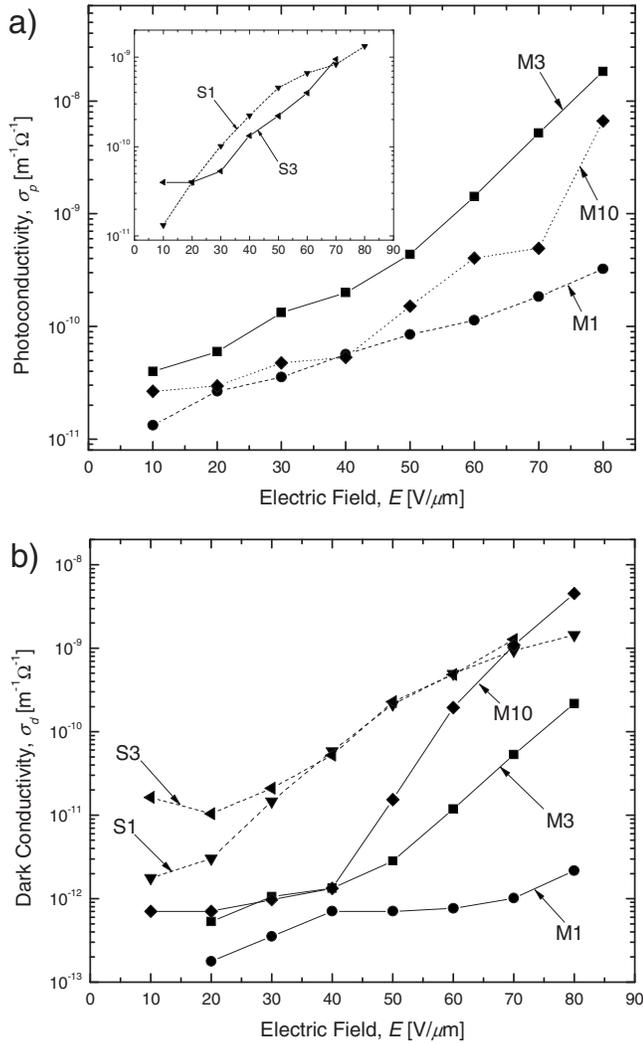
FIG. 7. (a) PC, σ_p and (b) dark-conductivity, σ_d, as a function of the externally applied electric field, E. The lines are guides for the eye.

sensitized composites and those photosensitized with PVK-SWCNT. In looking at the figure, it is apparent that under the employed I, M1, and M3 exhibit nearly identical σ_p/σ_d. Furthermore, this ratio remains nearly constant ($\sim$100 for the current I) across the entire range of E investigated. As the concentration of PVK-MWCNT is increased to that in M10, the σ_p/σ_d becomes more erratic but generally decreases relative to those observed for M1 and M3, especially at higher E. S1 and S3 exhibit a significantly diminished σ_p/σ_d compared to M1 and M3 ($\sim$1–10 with a comparable I). Similar to that of M10, though to a lesser degree, σ_p/σ_d for S1 and S3 seems to decrease as E is increased. While these data lend insight into the difference in PR performance between devices photosensitized with PVK-MWCNT and those sensitized with PVK-SWCNT, it is illustrative to analyze the σ_p and σ_d individually.

The σ_p and σ_d are presented in Fig. 7. Looking initially at the σ_p in Fig. 7(a) for M1 and M3, it is observed that an increase in the PVK-MWCNT corresponds to increase in σ_p, however evident from Fig. 7(b) is that a proportionately similar increase in σ_d is also observed. As was seen in Fig. 6, this trend is observed for the entire range of E relevant to this

study. The increase in the PVK-MWCNT concentration in going from M3 to M10 also begets the expected increase in the σ_d, but in this case, the σ_p does not incur a corresponding increase. As seen in Fig. 6, this is especially true at higher E. From these data, we conclude that once aggregation of the PVK-MWCNT begins to occur, increasing the concentration of the photosensitizer results in an increase in σ_d but any increase in σ_p is relatively meager, detrimentally affecting the PR performance. A similar behavior is observed for PR devices photosensitized with PVK-SWCNTs. However, here it is interesting that increasing the concentration of PVK-SWCNT in going from S1 to S3 does not result in a significant increase in σ_d. The reason for this apparent saturation is not immediately obvious but may be related to a percolation threshold. This behavior will be the subject of future experimentation.

Comparing σ_d, of M1 with that of S1, it is apparent that, unlike the σ_p which was nearly identical between the two composites, the σ_d of S1 exceeds that of M1 by three to four orders of magnitude. Although it has not yet been confirmed experimentally, it is speculated that this difference is likely due to the much larger number density of CNTs per unit volume in the S1 composite as compared to the M1 composite. The difference originates for two reasons; first, even though M1 and S1 have approximately the same α_{633}, a larger weight percentage of SWCNT was required to achieve this same α_{633}. Second, due to the "packing" which defines MWCNTs, a single MWCNT can be thought of as being composed of several "SWCNTs," therefore the number density per unit volume of MWCNTs will be lesser than that associated with an equal mass of SWCNTs. Combining both of these considerations leads to the conclusion that the number density per unit volume of SWCNT is going to be greatly increased relative to that of MWCNT to achieve the same α_{633}. As it is well known that CNTs are able to partake in charge-transport as well as charge-generation, in this case this extra contribution to charge-transport stemming from the relatively high concentration of SWCNTs translates into an increased σ_d.

In addition to the usual oxidative impurities, polymeric imperfections, etc., it is likely that PVK-CNTs can also contribute to the effective trapping of free charge-carriers. The trap densities for the composites could be relatively gauged by calculating the phase shift, ϕ, between the illumination pattern associated with the intersecting writing beams and the PR space-charge field. Here it is assumed that ϕ is inversely related to the trap density. This correlation is based on the assumption that an increase in the trap density would prevent free charges, in the form of photo-generated holes, from migrating fully into the dark regions of the illumination pattern. As the holes become dynamically fixed over a relatively shorter distance, ϕ will deviate from the theoretical maximum value of 90°. To calculate the phase shift, it is possible to first determine the change in refractive index with respect to p-polarized probe-beam used in the DFWM experiment, Δn, using the equation[42]
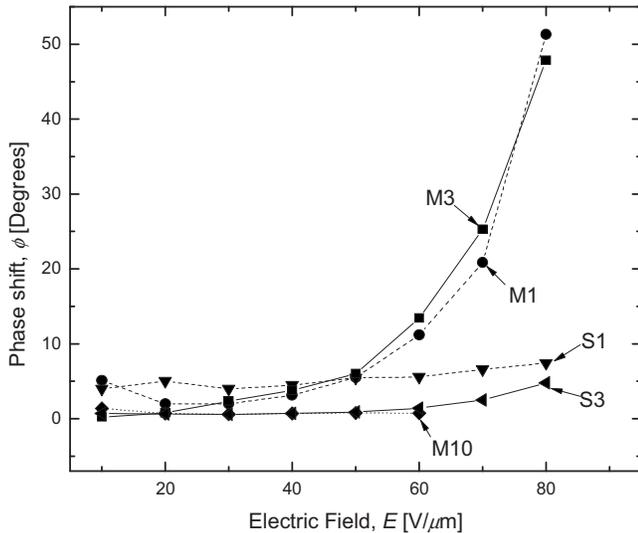
FIG. 8. Phase shift between illumination pattern and the space charge field, ϕ, as a function of the externally applied electric field, E. The lines are guides for the eye.

$$\eta_{int} = \sin^2\left[\frac{2\pi\Delta n d}{\lambda(\cos\theta_1 + \cos\theta_2)}\right]. \tag{8}$$

See Ref. 43 for the Δn as a function of E. These data were then employed in estimating ϕ according to the equation[42]

$$\phi = \sin\left(\frac{\Gamma\lambda}{2\pi\Delta n}\right), \tag{9}$$

which are plotted as a function of E in Fig. 8. As described, this parameter can provide qualitative insight with regard to the trap concentration. In Fig. 8, it is immediately apparent that for M1 and M3, ϕ remains nearly identical across the range of E investigated. Similarly, S1 and S3 also exhibit nearly identical values of ϕ across the range of E, though significantly decreased relative to those measured for M1 and M3. These data clearly show a significant difference between the achieved ϕ when PVK-MWCNT and when PVK-SWCNT are employed as the photosensitizer. Since this dramatic difference is observed even at relatively low concentrations, where aggregation is insignificant, such as those present in M1 and S1, the difference is inherent to the different CNTs, or to the degree to which the respective CNTs could be successfully adorned with PVK. Specifically, the data suggest that the PVK-SWCNT have a much higher propensity for the trapping of photo-generated charge carriers, holes in this case. It is also noted, in looking at the data obtained for M10, that as aggregation becomes significant, the propensity of the PVK-MWCNT to behave as a trapping species also increases greatly. This behavior is also apparent in that the slightly scattering S3 exhibits a small decrease in ϕ in comparison to the nonscattering S1.

IV. SUMMARY AND CONCLUSION

In conclusion, it has been demonstrated that the covalent bonding of CNTs to a charge-mediating species, such as PVK, results in a high performance PR composite. It has been established that the improvement in solubility of the CNT is the primary reason for the observed enhancement in PR performance. It has been further confirmed that, for the particular coupling scheme studied in this work, the grafting of the PVK to the MWCNTs is much more effective than was the case for the SWCNTs, resulting in PR composites with superior PR performance. Specific differences in the PR performance were observed, such as large and distinct differences in σ_p/σ_d as well as in ϕ, the origin and further implications of which will be subject of future studies. Also the subject of future studies will be the use of PVK-CNT as a photosensitizer at IR wavelengths. It is anticipated that many of the tendencies observed at $\lambda = 633$ nm will also be applicable at other wavelengths of interest such as 1310 and 1550 nm. A detailed study concerning the energetics of the relevant components will also be useful in formulating subsequent composites for particular applications.

[1]Y. Liu, S. Lu, and B. Panchapakesan, Nanotechnology **20**, 035203 (2009).
[2]H.-X. Wu, X.-Q. Qiu, R.-F. Cai, and S.-X. Qian, Appl. Surf. Sci. **253**, 5122 (2007).
[3]S. Lu and B. Panchapakesan, Nanotechnology **17**, 1843 (2006).
[4]L. Valentini, F. Mengoni, I. Armentano, J. M. Kenny, L. Ricco, J. Alongi, M. Trentini, S. Russo, and A. Mariani, J. Appl. Phys. **99**, 114305 (2006).
[5]R. F. Khairoutdinov, L. V. Doubova, R. C. Haddon, and L. Saraf, J. Phys. Chem. B **108**, 19976 (2004).
[6]W. Wu, S. Zhang, Y. Li, J. Li, L. Liu, Y. Qin, Z.-X. Guo, L. Dai, C. Ye, and D. Zhu, Macromolecules **36**, 6286 (2003).
[7]M. Freitag, Y. Martin, J. A. Misewich, R. Martel, and P. Avouris, Nano Lett. **3**, 1067 (2003).
[8]C. Li, C. Liu, F. Li, and Q. Gong, Chem. Phys. Lett. **380**, 201 (2003).
[9]W. Wu, J. Li, L. Liu, L. Yanga, Z.-X. Guo, L. Dai, and D. Zhu, Chem. Phys. Lett. **364**, 196 (2002).
[10]L. Liu, S. Zhang, T. Hu, Z.-X. Guo, C. Ye, L. Dai, and D. Zhu, Chem. Phys. Lett. **359**, 191 (2002).
[11]Y.-P. Sun, K. Fu, Y. Lin, and W. Huang, Acc. Chem. Res. **35**, 1096 (2002).
[12]M. J. O'Connell, S. M. Bachilo, C. B. Huffman, V. C. Moore, M. S. Strano, E. H. Haroz, K. L. Rialon, P. J. Boul, W. H. Noon, C. Kittrell, J. Ma, R. H. Hauge, R. B. Weisman, and R. E. Smalley, Science **297**, 593 (2002).
[13]P. Chen, X. Wu, X. Sun, J. Lin, W. Ji, and K. L. Tan, Phys. Rev. Lett. **82**, 2548 (1999).
[14]Photorefractive Materials and Their Applications, I and II, Topics in Applied Physics Vols. 61 and 62, edited by P. Gunter and J.-P. Huignard (Springer-Verlag, Berlin, 1988).
[15]P. Yeh, Introduction to Photorefractive Nonlinear Optics (Wiley, New York, 1993).
[16]O. Ostroverkhova and W. E. Moerner, Chem. Rev. **104**, 3267 (2004).
[17]J. Thomas, R. A. Norwood, and N. Peyghambarian, J. Mater. Chem. **19**, 7476 (2009).
[18]S. Köber, F. Gallego-Gomez, M. Salvador, F. B. Kooistra, J. C. Hummelen, K. Aleman, S. Mansurova, and K. Meerholz, J. Mater. Chem. **20**, 6170 (2010).
[19]T. V. Krivenko, L. Y. Pereshivko, A. D. Grishina, V. V. Savel'ev, R. W. Rychwalski, and A. V. Vannikov, High Energy Chem. **43**, 540 (2009).
[20]A. D. Grishina, L. Y. Pereshivko, T. V. Krivenko, V. V. Savel'ev, L. Licea-Jiménez, R. W. Rychwalski, and A. V. Vannikov, High Energy Chem. **42**, 543 (2008).
[21]L. Y. Pereshivko, A. D. Grishina, T. V. Krivenko, V. V. Savelev, and A. V. Vannikov, Mol. Cryst. Liq. Cryst. (Phila. Pa.) **496**, 293 (2008).
[22]A. D. Grishina, L. Y. Pereshivko, L. Licea-Jiménez, T. V. Krivenko, V. V. Savel'ev, R. W. Rychwalski, and A. V. Vannikov, High Energy Chem. **41**, 267 (2007).

[23] L. Licea-Jiménez, A. D. Grishina, L. Y. Pereshivko, T. V. Krivenko, V. V. Savel'ev, R. W. Rychwalski, and A. V. Vannikov, Carbon **44**, 113 (2006).

[24] A. D. Grishina, L. Licea-Jiménez, L. Y. Pereshivko, T. V. Krivenko, V. V. Savel'ev, R. W. Rychwalski, and A. V. Vannikov, High Energy Chem. **40**, 341 (2006).

[25] A. V. Vannikov, R. W. Rychwalski, A. D. Grishina, L. Y. Pereshivko, T. V. Krivenko, V. V. Savel'ev, and V. I. Zolotarevski, Opt. Spectrosc. **99**, 643 (2005).

[26] A. Maity and S. S. Ray, Synth. Met. **159**, 1158 (2009).

[27] A. Maity, S. S. Ray, and M. J. Hato, Polymer **49**, 2857 (2008).

[28] A. Maity and M. Biswas, J. Appl. Polym. Sci. **104**, 4121 (2007).

[29] W. Wang, Y. Lin, and Y.-P. Sun, Polymer **46**, 8634 (2005).

[30] C. Wang, Z.-X. Guo, S. Fu, W. Wu, and D. Zhu, Prog. Polym. Sci. **29**, 1079 (2004).

[31] M. A. Díaz-García, D. Wright, J. D. Casperson, B. Smith, E. Glazer, W. E. Moerner, L. I. Sukhomlinova, and R. J. Twieg, Chem. Mater. **11**, 1784 (1999).

[32] P. Magdolen, M. Mečiarová, and Š. Toma, Tetrahedron **57**, 4781 (2001).

[33] J. Thomas, C. Fuentes-Hernandez, M. Yamamoto, K. Cammack, K. Matsumoto, G. A. Walker, S. Barlow, B. Kippelen, G. Meredith, S. R. Marder, and N. Peyghambarian, Adv. Mater. **16**, 2032 (2004).

[34] J. Ostrauskaite, H. R. Karickal, A. Leopold, D. Haarer, and M. Thelakkat, J. Mater. Chem. **12**, 3469 (2002).

[35] D. Wright, U. Gubler, W. E. Moerner, M. S. DeClue, and J. S. J. Siegel, J. Phys. Chem. B **107**, 4732 (2003).

[36] G. B. Jung, M. Yoshida, T. Mutai, R. Fujimura, S. Ashihara, T. Shimura, K. Araki, and K. Kuroda, Sen'i Gakkaishi **60**, 193 (2004).

[37] C. Fuentes-Hernandez, J. Thomas, R. Termine, G. Meredith, N. Peyghambarian, and B. Kippelen, Appl. Phys. Lett. **85**, 1877 (2004).

[38] S. Tay, J. Thomas, M. Eralp, G. Li, R. A. Norwood, A. Schülzgen, M. Yamamoto, S. Barlow, G. A. Walker, S. R. Marder, and N. Peyghambarian, Appl. Phys. Lett. **87**, 171105 (2005).

[39] M. Eralp, J. Thomas, G. Li, S. Tay, A. Schülzgen, R. A. Norwood, N. Peyghambarian, and M. Yamamoto, Opt. Lett. **31**, 1408 (2006).

[40] M. Eralp, J. Thomas, S. Tay, G. Li, A. Schülzgen, R. A. Norwood, M. Yamamoto, and N. Peyghambarian, Appl. Phys. Lett. **89**, 114105 (2006).

[41] W. E. Moerner and S. M. Silence, Chem. Rev. **94**, 127 (1994).

[42] R. Bittner, K. Meerholz, G. Steckman, and D. Psaltis, Appl. Phys. Lett. **81**, 211 (2002).

[43] See supplementary material at http://dx.doi.org/10.1063/1.3530583 for a plot of the Δn as a function of E.